

Beam Based Alignment Procedure for an Undulator with Superimposed FODO Lattice

K. Flöttmann, B. Faatz, E. Czuchry and J. Roßbach

1 Introduction

The aim of beam based alignment techniques is to determine the relative offset between a beam position monitor (BPM) and the magnetic axis of a quadrupole (or sextupole) magnet by means of beam observations. While the offset information can be used to improve the mechanical alignment of accelerator components (e.g. with micro movers) it is often sufficient or even equivalent to correct the alignment errors by means of corrector magnets, i.e. the offset information is the basis for improved trajectory corrections. Therefore beam based alignment procedures mediate between classical accelerator alignment and orbit correction techniques.

Different beam based alignment methods have been developed for linear accelerators [2] and for circular machines [3]. The primary goal of these techniques, however, is not to keep the beam on a given orbit, but to minimize distortions that result from orbit deviations, for example emittance dilution. On the contrary, in case of the FEL the aim is to keep the beam on a straight line in order to maximize the interaction of the photon field with the electron beam. According to simulation studies [4] the rms orbit deviation of the electron beam with respect to a straight line has to be below $10\ \mu\text{m}$ at least over the length of one undulator module (4.5m). The planar undulator consists of a conventional permanent magnet structure with superimposed permanent magnet quadrupoles, which are expected to be the dominating source for orbit kicks [5]. Beam Position Monitors (BPMs) and corrector magnets will be integrated into the vacuum chamber of the undulator in order to allow for a correction of the orbit. Table 1 summarizes relevant parameters of the undulator and the beam optics. Since the quadrupoles are made of permanent magnets they are fixed in strength and position. Besides the strength of individual corrector magnets only the beam energy can be changed. With respect to beam optics, this is equivalent to changing the strength of all magnets simultaneously. Unfortunately the betatron phase advance inside the quadrupole magnets is rather large, i.e. it is not valid to simplify the problem by means of a thin lens

Table 1
Undulator and optics parameters for the TTF FEL (Phase I) [1].

undulator	
number of modules	3
length of module	4.5 m
period length	27.3 mm
undulator peak field	0.5 T
rms field error $\Delta B/B$	$< 4 \times 10^{-3}$
number of quadrupoles per module	10
length of quadrupoles	136.5 mm
distance between quadrupoles	341 mm
offset error	$< 50 \mu\text{m}$
corrector length	300 mm
integrated strength	2.5 T
focal length	0.4 m (at 300 MeV)
optics (at 300 MeV)	
β_{max}	1.5 m
β_{min}	0.5 m
phase advance per FODO cell	65°
betatron wavelength	$\approx 6.3 \text{ m}$

approximation. Additional constraints arise from random dipole errors generated by the undulator and the very tight tolerances for the overlap of the electron beam with the radiation field in case of an FEL.

This paper presents a detailed discussion of a local correction procedure while a global procedure is discussed in Ref. [6]. A comparison of both methods is found in Ref. [7]. It should be noted that alternative approaches for the alignment problem, using for example synchrotron radiation, are under consideration which will not be discussed here (see Ref. [8]). In the following we will concentrate on the case of a low beam energy of 300 MeV (Phase I of the FEL experiment) since the situation is more relaxed at higher beam energies.

2 Orbit Deviation due to Uncorrelated Quadrupole Magnet Misalignments

If a quadrupole magnet lattice is superimposed to the undulator, the orbit distortion due to random field errors grows in a significantly different way. Due to the presence of focussing fields, there will be a tendency to bend the distorted orbit back to the axis, resulting in a much slower growth of the distortion's amplitude. This effect sets in after approx. $\mu = \pi/2$ betatron phase advance. Thus, the tolerances on field errors have to be determined in a different way if the level of tolerable orbit distortion is exceeded within $\mu < \pi/2$ (i.e. before focussing becomes effective) or if not.

Consider the orbit displacement due to N dipole kicks. In the following we assume that these kicks are generated by quadrupole misalignments δx_i (a generalization is simple). With s being the longitudinal coordinate and f_i the focal length of the i th quadrupole, the orbit displacement is given by

$$\Delta x(s) = \sum_i \frac{\delta x_i}{f_i} \sqrt{\beta_i \beta(s)} \sin(\mu(s) - \mu_i) = \sum_i \frac{\delta x_i}{f_i} \beta \sin(\mu(s) - \mu_i)$$

where the latter equality makes use of a smooth focussing approximation and β is the beta-function. Since we do not know the specific error distribution, we can only perform a statistical analysis. Assuming, for simplicity, a periodic FODO lattice with equal focal length f of all quadrupoles and uncorrelated errors, the mean squared orbit distortion at longitudinal position s is given by

$$\begin{aligned} \langle (\Delta x(s))^2 \rangle &= (x_{\text{rms}}(s))^2 = \frac{\beta^2}{f^2} \langle \sum_i \delta x_i^2 \rangle \langle \sin^2(\mu(s) - \mu_i) \rangle \\ &= N \frac{\beta^2}{f^2} (\sigma_q)^2 \left(\frac{1}{2} - \frac{\sin 2\mu(s)}{4\mu(s)} \right) \end{aligned}$$

For a lattice with small betatron phase advance per FODO cell $\mu_{\text{cell}} < \pi/2$ we can write (l_d is the drift space between quadrupole lenses, – we use thin lens approximation)

$$\sin\left(\frac{\mu_{\text{cell}}}{2}\right) = \frac{l_d}{2f} \approx \frac{\mu_{\text{cell}}}{2} \quad \text{and} \quad \frac{\beta}{f} \approx 2$$

Thus

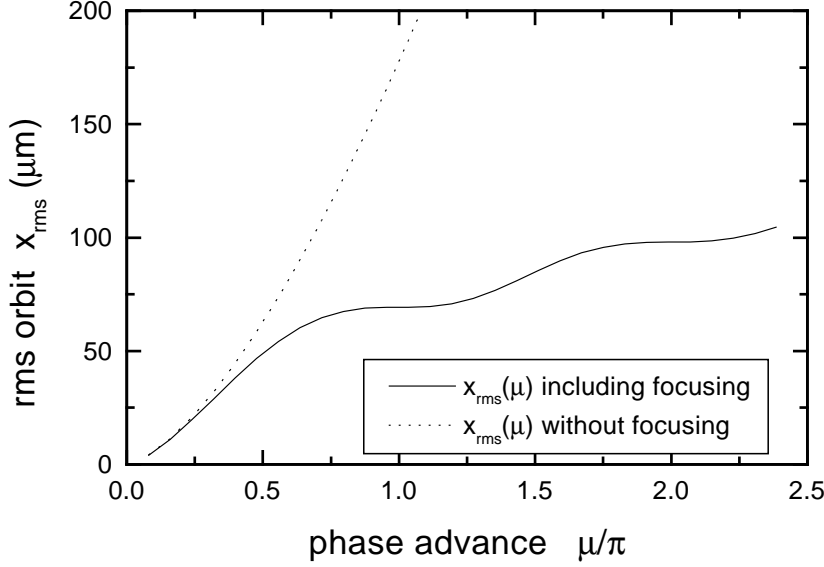


Fig. 1. Orbit deviation due to errors with (solid line) and without focusing (dotted line). The phase advance μ_{cell} per cell has been chosen equal to $\pi/3$ and the quadrupole misalignment $20 \mu\text{m}$.

$$x_{\text{rms}}(s) = \sigma_q \left[\left(1 - \frac{\sin 2\mu(s)}{2\mu(s)} \right) \frac{4\mu(s)}{\mu_{\text{cell}}} \right]^{1/2} \quad (1)$$

For $\mu(s) \gg \pi$, this scales like $(x_{\text{rms}}(s)) \propto \sqrt{\mu(s)} \propto \sqrt{s}$, while for $\mu(s) \ll \pi$:

$$x_{\text{rms}}(s) \approx \sigma_q \left[\frac{8\mu(s)^3}{3\mu_{\text{cell}}} \right]^{1/2} \propto \mu(s)^{3/2} \propto s^{3/2} \quad (2)$$

It is easy to see that this latter case is equivalent to the case of *no* focussing:

$$x_{\text{rms}}(s) = \left[\left\langle \sum_{i=1}^N i^2 l_d^2 \frac{\delta x_i^2}{f^2} \right\rangle \right]^{1/2} = \sqrt{\frac{N^3}{3}} l_d \frac{\sigma_q}{f} = 2\sigma_q \left[\frac{2\mu(s)^3}{3\mu_{\text{cell}}} \right]^{1/2}$$

which is indeed identical to eq. 2.

Fig. 1 compares the case with focusing (Eq. 1) and the case without focusing (Eq. 2). The phase advance per FODO cell is $\pi/3$ and the quadrupole offsets are $20 \mu\text{m}$ rms. The specifications of the FEL are exceeded within the first FODO cell. Consequently, correctors are required within a cell, and with respect to the orbit correction one does not profit too much from the presence of focusing.

3 Modelling and Simulation of the Undulator

Based on the statistical arguments given in the previous section, one can estimate the minimum number of correctors needed to keep the rms orbit deviation within the required tolerance of $10\ \mu\text{m}$ to be one per FODO cell. In general one will need more correctors in order to compensate for additional errors, i.e. BPM offsets which are not taken into account in the previous estimation. The procedure discussed in the following requires one BPM and one corrector per quadrupole. A reduction of both elements is possible with the global procedure (Ref. [6]) only. In order to simulate possible procedures of alignment, a computer code has been developed. It contains the following features.

- **Beam position monitors.** The BPMs have no longitudinal extension in the code. They have a random offset and a given resolution. Note, that in reality the BPMs consist of two elements which are longitudinally separated by about 70 mm because of the geometrical constraints in the undulator gap. The total space needed per BPM is approximately 110 mm.
- **Corrector coils.** In the code, correctors can have an arbitrary position and strength. The length of the corrector is 300 mm. A minimal distance of ≈ 55 mm between the BPM center and the corrector entrance is required in reality due to the finite BPM length, space for cabling etc.
- **Dipole errors.** The ideal undulator field is sinusoidal. In addition to that ideal field, random peak field errors are added each half period. This is only consistent with Maxwells equations on the optical axis. In order to include magnetic field correction procedures, the second field integral can be corrected over an arbitrary distance.
- **Quadrupole misalignment.** The quadrupoles can have an arbitrary misalignment in x or y direction by adding a homogeneous random displacement within predefined boundaries. A longitudinal displacement or an error in quadrupole gradient has not been included. The quadrupoles are assumed to have ‘hard edges’, i.e. the field goes to zero instantaneously at the entrance/exit of the quadrupoles. A thin lens approximation is not used. *

The length of correctors and quadrupoles are given in terms of half undulator periods (therefore the thin quadrupole lens can be approximated by taking this minimum length and adjusting the gradient to obtain the same focal length). Although quadrupole lengths and positions as well as BPM and corrector position can be chosen arbitrarily in the code, the simulations performed here only

* If the focal length of the quadrupole lens is much larger than its geometrical length, the phase advance in the magnet is small and the lens can be described using only linear dispersion. In this description, the lens has no geometrical length and the beam is kicked with a strength inversely proportional to the energy of the beam and independent of the incoming beam angle.

include periodic structures. Furthermore, it is assumed that the two transverse planes can be described independently and only the wiggling plane is studied. A schematic layout of the features included in the program is shown in Fig. 2.

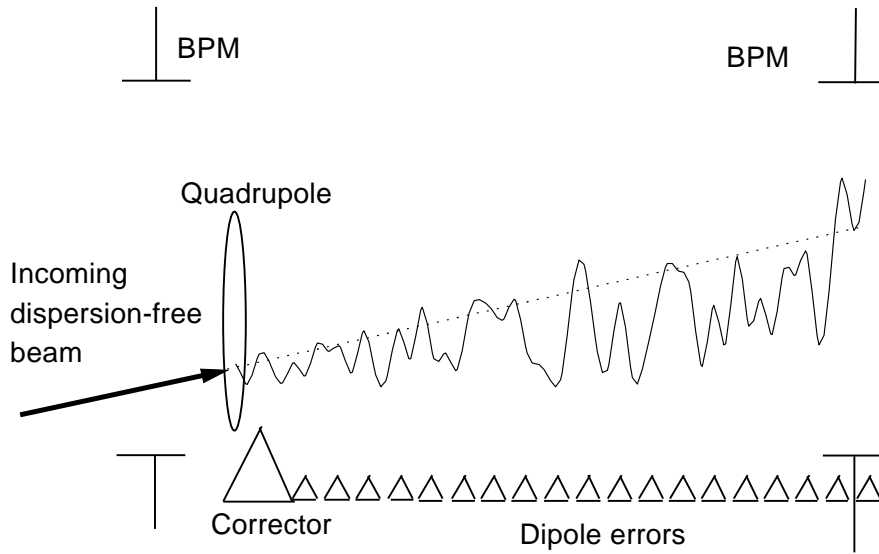


Fig. 2. A schematic overview of the beam based alignment procedure described in this paper. At the BPM positions, the beam continues in the direction of the incident beam. In between, there are deviations due to the undulator (dipole) peak field errors.

4 The Algorithm

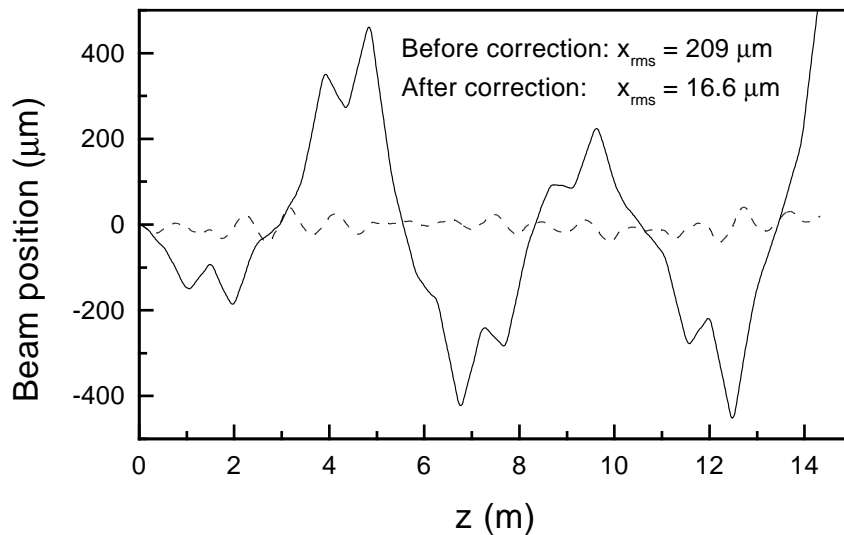


Fig. 3. Example of a beam trajectory before (solid line) and after correction (dashed line). The rms orbit is $16.6\mu\text{m}$ after correction.

Since no external reference line exists for the beam based alignment procedure the question arises to which line the beam can be aligned? The procedure

discussed below forces the beam onto the extrapolation of the incoming beam trajectory. Thus the straight line is defined by the position and angle of the incoming beam (see Fig. 2). At the end of section 5 it will be shown how the incoming beam position and angle can be corrected, so that the beam passes through the average quadrupole axis. The beam with initial conditions x_0 and x'_0 at the entrance of the undulator is given in the thin lens approximation by:

$$x_1 = x_0 + x'_0 \cdot s + \frac{K_q}{p} \cdot s_q + \sum_i \frac{D_i}{p} \cdot s_i + \frac{C}{p} \cdot s_c \quad (3)$$

at the next BPM. Here K_q/p is the kick generated by the quadrupole, D_i/p are the dipole kicks and C/p is the kick of the corrector. The momentum of the beam is denoted by p and s_q , s_i and s_c indicate the distance from the element to the BPM. Note, that K_q is independent of energy only if the position and, in case of a thick lens, also the angle of the beam at the quadrupole do not change with energy (see Fig. 2). At the entrance of the undulator this can easily be achieved by means of two BPMs and two correctors which allow to decouple the dispersion generated in the undulator from the dispersion generated upstream in the linac. However, rather than using the correctors for a correction of the incoming dispersion and hereby fixing the beam angle and position at the undulator entrance, the excitation of the correctors will be changed when the energy is changed so that an arbitrary position and angle can be realized with a dispersion free behaviour. In order to reduce Eq. (3) to: $x_1 = x_0 + x'_0 \cdot s$, i.e. to force the trajectory onto the extrapolation of the incoming beam trajectory the sum of all kicks, weighted with the distance to the next BPM, has to be zero. Obviously this is the case when the measured beam position at the next BPM is independent of the beam energy. If the BPM is located at the next quadrupole, Eq. (3) applies for the next section with K_q being independent of energy. Therefore the beam can be forced onto a straight line at the positions of the BPMs if a BPM is located at each quadrupole and one corrector per quadrupole is available. (It will, of course, deviate from a straight line in between the BPMs.) Note that while the position at the BPMs is independent of energy the angle will in general slightly change when the energy is changed. The variations of the beam angle in conjunction with the thick lens behaviour lead to a slow drift from a straight line which is typical for local alignment procedures. This bowing has no significant influence on the FEL performance, since the drift length is large compared to the gain length in most cases. In section 5 a possible correction procedure is discussed.

A simple way to determine the required excitation of the corrector coil is to measure the beam position at the next BPM as function of the excitation for two different energies (typically with 10% energy variation). The intersection of both measured lines indicates the required corrector setting. The lines can be determined with very high accuracy even if the BPM resolution is not very

good by taking more measurement points.

Since the beam is forced to follow the incoming beam vector its trajectory can in principle be far off axis at the end of the undulator. In this case, the corrector settings will show a linear growing amplitude in order to compensate the quadrupole orbit kicks. Therefore, a beam trajectory far off axis can be detected and corrected in a second step. Similarly, it is also possible to identify misaligned individual undulator modules (see Fig. 10), i.e. one gets relevant information for mechanical realignment.

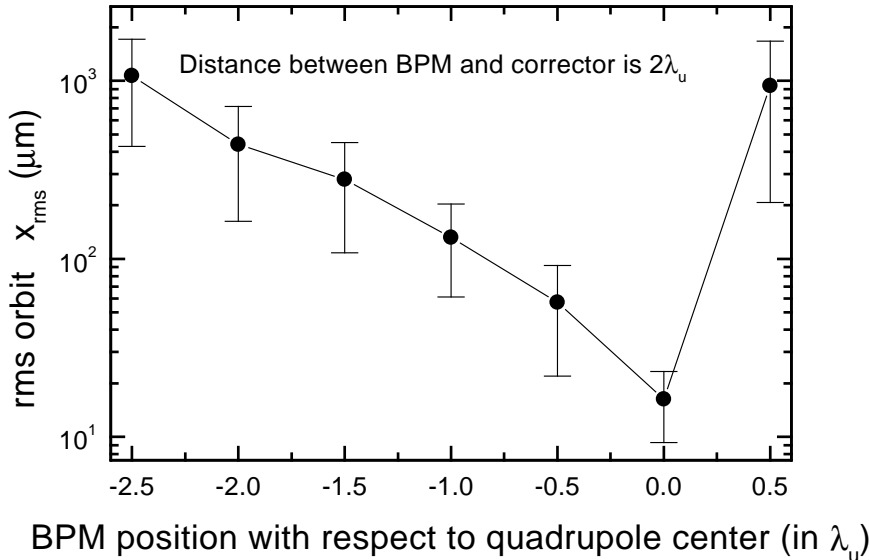


Fig. 4. The rms orbit averaged over 100 samples as a function of position of the BPMs with respect to the quadrupole center. The distance between BPM and corrector entrance is two undulator periods in all cases, the BPMs are assumed to have perfect resolution. The second field integral has been corrected along the undulator axis every 10 undulator periods. The energy difference in order to measure the dispersion has been chosen equal to 10%.

Fig. 3 shows as an example a beam trajectory before and after correction. The rms orbit is $16.6 \mu\text{m}$. In the following, the influence of the longitudinal BPM position (relative to the quadrupole position), the BPM resolution and the corrector position will be discussed. In the simulations of which results are shown each point represents the average and standard deviation of 100 random seeds, respectively.

5 Results of simulations.

The first set of simulations (see Fig. 4), determines the optimum position of the BPM with respect to the center of each quadrupole. The space needed for the beam position monitors is approximately 110 mm. Therefore, the distance

between BPM and corrector has always been chosen equal to two undulator periods, i.e. BPM and corrector are shifted as a block with respect to the quadrupole. The minimum rms orbit always occurred with the BPM at the quadrupole center. The minimum values varied between 8 and 30 μm for a beam energy of 300 MeV. Correcting the second field integral did not only reduce the required corrector strength, but in those cases where the rms orbit was still large, this value was also significantly reduced.

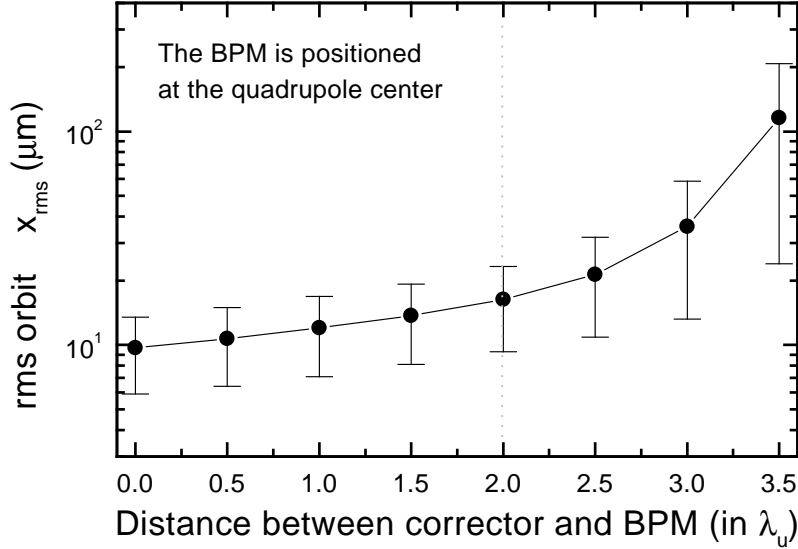


Fig. 5. The rms orbit as a function of distance between BPMs and correctors. A distance of zero corresponds to the case when the corrector starts at the BPM position, which is taken at the quadrupole center in all cases. A distance of two undulator periods corresponds to the TTF case. The second field integral has been corrected along the undulator axis every 10 undulator periods. The energy difference used to measure the dispersion has been chosen equal to 10%. The dotted line indicates the nominal distance between BPM and corrector.

Although the distance between BPM and corrector cannot become zero, because a certain amount of space is needed for connections etc., it is important to see what amount of reduction of rms orbit could be achieved if one would put effort in reducing the distance between corrector and BPM below $2\lambda_u$. Results are shown in Fig. 5. Reducing the distance to values smaller than the two undulator periods assumed in the previous calculations does give a further reduction. However, if the rms orbit is already small, the additional reduction is moderate, while an increased distance leads to significantly poorer results.

Fig. 6 shows a histogram of 1000 random distributions of quadrupole offsets and dipole field errors. The BPMs are located in the quadrupole center and the distance between corrector and BPM is $2\lambda_u$. The mean value, 16 μm in this case, does not correspond to the value with the highest probability (12 μm).

The corrector strength needed for the case with the BPM in the quadrupole center and the distance between BPM and corrector entrance of two undulator

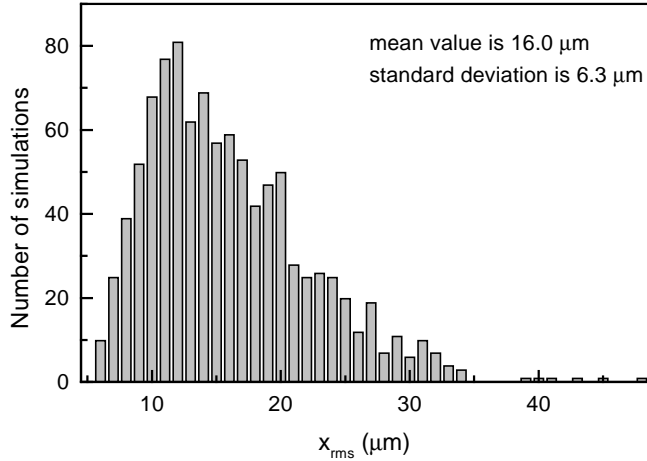


Fig. 6. Histogram showing the rms orbit of 1000 samples of random dipole errors, quadrupole displacement and BPM offsets. All remaining simulations have been performed with 100 samples out of these one thousand, giving approximately the same average rms orbit.

periods is shown in Fig. 7. The most obvious result is an increase of the corrector strength along the undulator. This effect, as well as the increasing of the rms orbit when the distance between BPM and corrector is increased, is caused by the bowing of the trajectory due to the variation of the beam angles at the quadrupoles as discussed in section 4. It can be minimized by putting correctors on top of the quadrupoles, so that the dominant kicks are locally compensated and the angles are reduced.

In Fig. 8, a result is shown when the corrector has the same length as the quadrupole and they completely overlap. This is equivalent to the case where the quadrupoles can be moved with micro movers. The BPM is positioned at the quadrupole entrance. The second field integral has been corrected every 5 undulator periods. In case of correction every 10 periods, the quadrupole

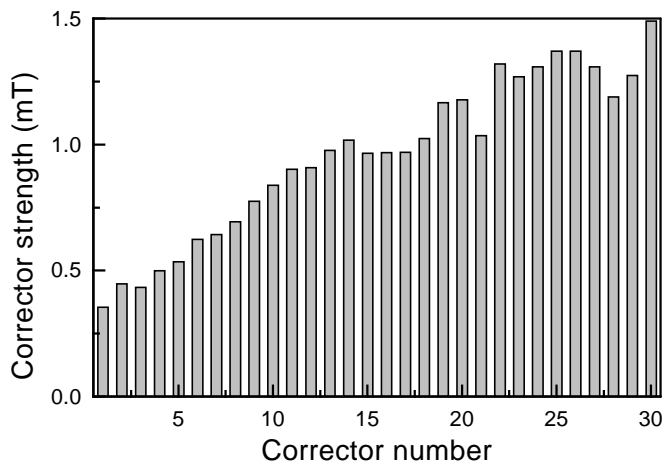


Fig. 7. Corrector strength needed to get the beam on axis for a displacement of quadrupoles of $50 \mu\text{m}$ and an incoming beam being perfectly on axis.

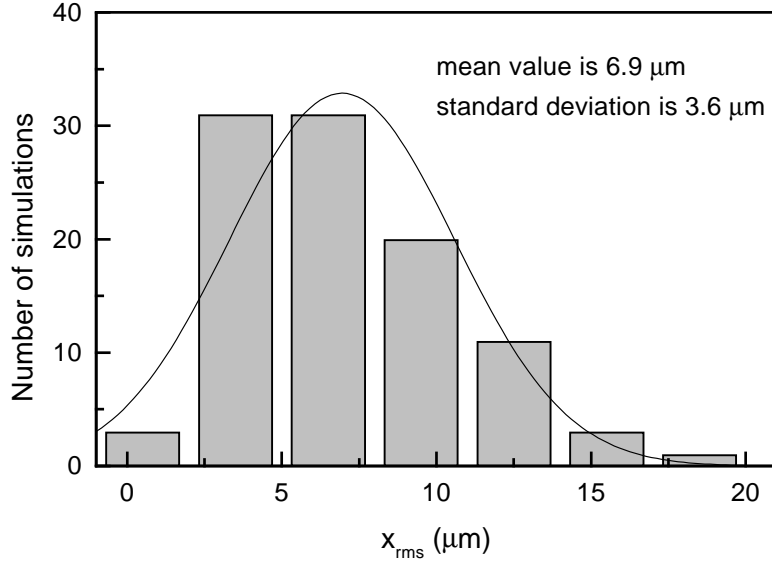


Fig. 8. Histogram showing simulation results with correctors completely overlapping the quadrupoles. The second field integral has been corrected every 5 undulator periods. The energy difference chosen to measure the dispersion has been chosen equal to 10%.

displacement does not dominate the dispersion enough to show a significant decrease in the rms orbit. The mean value is reduced to $7 \mu\text{m}$, thus the procedure is limited in case of the TTF-FEL by the fact that weak and rather long correctors do not overlap with the quadrupoles. This leads to energy dependent angles in the quadrupoles, that act as thick lenses, and a deviation of the trajectory from the ideal straight line.

Simulations so far assumed a maximum quadrupole displacement of $\pm 50 \mu\text{m}$. Most likely, however, the alignment can be more accurate than this. With a smaller misalignment, the overall rms orbit decreases. Furthermore, the expected corrector strength becomes smaller. The smaller the effect of the dipole errors, the larger the reduction in the rms orbit. If the quadrupole misalignment is decreased from $\pm 50 \mu\text{m}$ to $\pm 10 \mu\text{m}$, the rms orbit reduces by about 20%. The current needed for the correction reduces by about the same amount. With the method described in this paper, a further reduction of the rms orbit is only possible by decreasing the effect of the dipole errors.

The results that have been shown so far involved perfect BPMs. Fig. 9 shows results of the influence of the BPM resolution on the rms orbit. There is a slight increase in the rms orbit, but this can in principle be compensated by taking more measuring points.

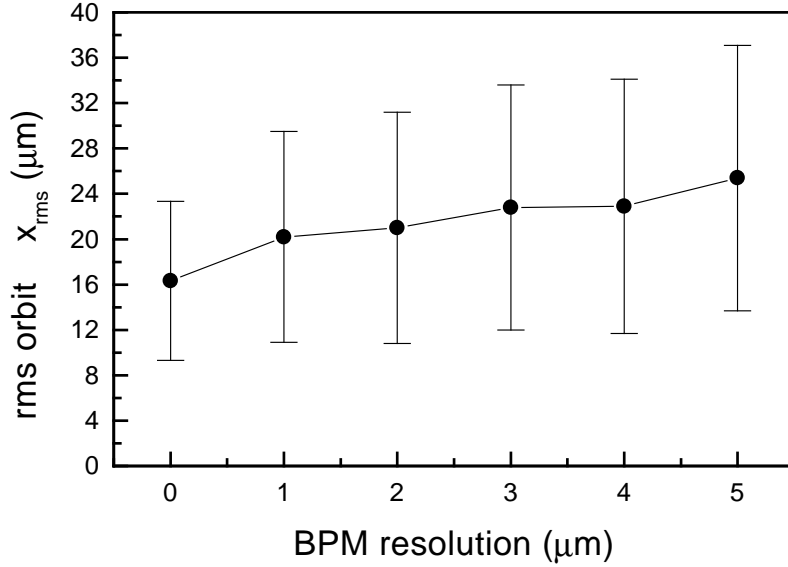


Fig. 9. rms orbit as a function of BPM resolution. The slight increase can be compensated by increasing the number of measurements. The second field integral has been corrected every 10 undulator periods. The energy difference used to measure the dispersion has been chosen equal to 30% for all but perfect BPMs.

Correction of incoming beam position and angle and module displacements.

The TTF FEL undulator consists of 3 modules each of 4.5m length (6 modules in the final version.) In order to assure an accurate alignment of the quadrupoles within each module (and also from one module to the next) a 12 m long measurement bench has been set up. Two neighboring modules will be measured at a time and alignment fiducials will guarantee a high alignment accuracy of the modules in the tunnel. Displaced modules may nevertheless lead to correlated quadrupole displacements. Since the modules will be mounted on micro movers their position can in principle be corrected remotely.

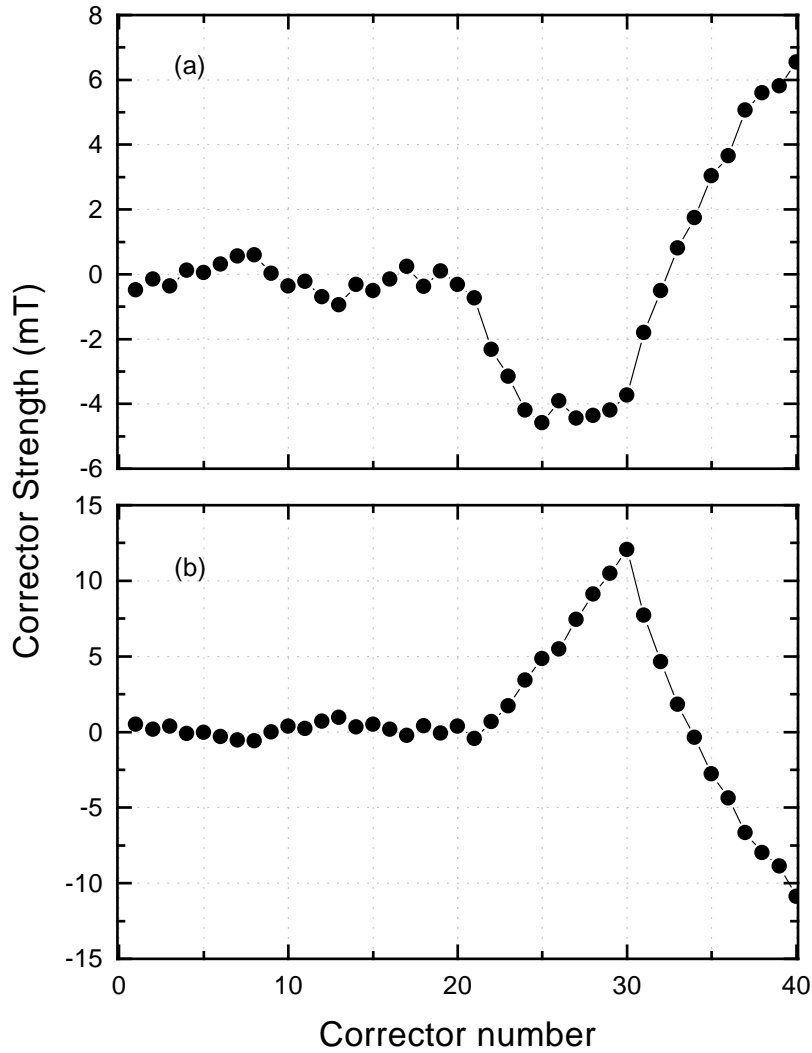


Fig. 10. *Corrector strength after beam based alignment procedure in case of a displaced module. The upper plot shows the effect of an offset of module 3 ($100\ \mu\text{m}$) and the lower plot shows the effect of an angle ($100\ \mu\text{rad}$). Module 3 extends from corrector 20 to 30. The linear correlated part of the corrector setting is clearly visible.*

The beam based alignment procedure forces the beam onto a straight line defined by the position and angle of the incoming beam. A displaced module shows up in the corrector settings as linearly correlated contribution of the normalized corrector strength. The normalized corrector strength is the corrector strength times -1 if the corrector is correcting a defocusing quad and times +1 if it is correcting a focusing quad, respectively. Figure 10 shows the corrector strength in case of a displaced module. The upper plot shows the effect of an offset of module 3 ($100\ \mu\text{m}$) and the lower plot shows the effect of an angle ($100\ \mu\text{rad}$) (Module 3 extends from corrector 20 to 30.) The linearly correlated contribution to the corrector setting gives a clear signal for the displacement of the module. Similarly the corrector settings show a linear behavior over the length of the whole undulator if the incoming beam has an angle or an

offset with respect to the average quadrupole position. Appropriate scaling factors between corrector setting and geometrical module displacement can be derived either from simulations or be determined experimentally, so that the incoming beam position and module displacements can be corrected.

Correlations similar to incoming beam errors can be generated by the beam based alignment procedure itself, since small variations of the beam angle at the entrance of the (thick lens) quadrupoles may lead to a slow orbit drift. Although this does not influence the FEL performance, since the drift length is large compared to the gain length in most cases, it is still useful to look at ways to compensate for this drift. One way is to use the correlations between corrector strength, as described before, another one is to use an independent measuring system, with only a few monitors along the entire undulator, which are referenced to an external measuring line. In case of the TTF-FEL, a wire scanner system with external reference marks between the undulator modules will allow to control the beam orbit independent of BPM's.

6 Discussion

Beam based alignment procedures can in general be affected by numerous error sources like:

- calibration (scaling) errors of the BPMs
- non-linearities of the BPMs
- calibration (scaling) errors of the corrector magnets
- hysteresis and saturation of the corrector magnets
- error accumulation in a long beam line
- incoming beam jitter
- motions due to temperature variations

Fortunately the algorithm does not rely on an accurate calibration of the BPMs and corrector magnets since no absolute measurements are required. In order to keep the effect of non-linearities of the BPMs small the scanning range has to be kept small. In the simulations the beam position in the BPMs were kept below ± 1 mm during the scanning procedure. It is expected that the BPMs are highly linear within this range. Saturation of the corrector magnets could be taken into account if it occurs but hysteresis would be a problem. Since the corrector magnets are basically air coils and the iron of the undulator surrounding the coils is highly saturated both effects should be negligible. Measurements to check the saturation and hysteresis effects are under preparation.

In the procedure each beam line element between two BPMs is corrected independently of all the others. The only assumption is that the incoming beam position is independent of the beam energy which can be checked within the accuracy of the BPMs at each position. In that sense no errors accumulate due to the procedure. The problem of correlated displacements of the quadrupoles (i.e. a displaced module) and/or an angle or offset of the incoming beam can be attacked by using a straight line fitting algorithm to the steerer strength after the first alignment procedure.

The jitter of the incoming beam is expected to be small. The effect of incoming beam jitter on the beam based alignment procedure is similar to the effect of noise in the electronics of the BPMs. It can be corrected by averaging over several shots. Since the BPM signals are digitized and hence limited in resolution a small noise level (of the order of the ADC resolution) is in general useful, since it allows to improve the measurement accuracy beyond the ADC resolution.

During the scanning procedure the rather weak corrector magnets will be excited to their maximum current. Since the correctors are integrated into the vacuum chamber the chamber will be heated which might eventually result in a motion of the neighboring BPM's. The scanning is, however, fast and the corrector windings are directly water cooled. In addition the mechanical design will minimize motions of the BPMs, so that the overall effect is expected to be negligible.

In conclusion it can be said that the discussed beam based alignment procedure is expected to be very robust and insensitive to most of the effects that can occur in a real accelerator environment. It complements a global alignment procedure which is described in Ref. [6].

References

- [1] *A VUV Free Electron Laser at the TESLA Test Facility: Conceptual Design Report*, DESY Print TESLA-FEL 95-03, Hamburg, 1995.
- [2] C.E. Adolphsen et. al., *Beam Based Alignment Technique for the SLC Linac* Proc. IEEE Particle Accelerator Conf., Chicago, 1989; and SLAC-PUB-4902 (1989).
T.O. Raubenheimer and R.D. Ruth, *A dispersion-free trajectory correction technique for linear colliders* Nucl. Instr. Meth. **A302** (1991) 191.
P. Tenenbaum, D. Burke, R. Helm, J. Irwin, P. Raimondi, K. Oide and K. Flöttmann, *Beam-Based Alignment of the Final Focus Test Beam*, SLAC-PUB-95-7058.

- [3] R. Brinkmann and M. Böge, *Beam Based Alignment and Polarization Optimization in the HERA Electron Ring*, Proc. at the EPAC 94, London, DESY Print M-94-03, 1994.
- [4] B. Faatz, J. Pflüger and Yu.M. Nikitina, *Study of the undulator specification for the VUV-FEL at the TESLA Test Facility*, Nucl. Instrum. Meth. **A393** (1997) 380.
- [5] J. Pflüger, Y. Nikitina, *Undulator Schemes with the Focusing Properties for the VUV- FEL at the TESLA Test Facility*, DESY Print TESLA-FEL 96-02, Hamburg 1996.
- [6] P. Castro, *TTF FEL Beam Based Alignment by Dispersion Correction using Micado Algorithm*, DESY Print TESLA-FEL 97-04, Hamburg 1997.
- [7] P. Castro, B. Faatz and K. Flöttmann, *Beam Based Alignment Procedure for an Undulator with Superimposed FODO Lattice*, presented at the FEL97 conference, Beijing, China, DESY Print TESLA-FEL 97-06, Hamburg 1997.
- [8] J.S.T. Ng, *A Beam Trajectory Monitor using Spontaneous Undulator Radiation*, DESY Print TESLA-FEL 96-16, Hamburg, 1996.